

RESEARCH LETTER

10.1002/2014GL060985

Key Points:

- The first direct constraints on strain accumulation within the Sea of Marmara
- Princes' Islands segment likely represents the most imminent danger
- The central Marmara segment is not accumulating strain at significant rates

Supporting Information:

- Readme
- Table S1
- Figure S1
- Figure S2

Correspondence to:

S. Ergintav,
semih.ergintav@boun.edu.tr

Citation:

Ergintav, S., R. E. Reilinger, R. Çakmak, M. Floyd, Z. Cakir, U. Doğan, R. W. King, S. McClusky, and H. Özener (2014), Istanbul's earthquake hot spots: Geodetic constraints on strain accumulation along faults in the Marmara seismic gap, *Geophys. Res. Lett.*, 41, 5783–5788, doi:10.1002/2014GL060985.

Received 25 JUN 2014

Accepted 7 AUG 2014

Accepted article online 11 AUG 2014

Published online 22 AUG 2014

Corrected 16 SEP 2014

This article was corrected on 16 SEP 2014.
See the end of the full text for details.

Istanbul's earthquake hot spots: Geodetic constraints on strain accumulation along faults in the Marmara seismic gap

S. Ergintav¹, R. E. Reilinger², R. Çakmak³, M. Floyd², Z. Cakir⁴, U. Doğan⁵, R. W. King², S. McClusky⁶, and H. Özener¹

¹Boğaziçi University, Department of Geodesy, Kandilli Observatory and Earthquake Research Institute, Istanbul, Turkey,

²Department of Earth, Atmospheric and Planetary Sciences, Massachusetts Institute of Technology, Cambridge, Massachusetts, USA, ³TUBITAK, MRC, Earth and Marine Sciences Institute, Kocaeli, Turkey, ⁴Istanbul Technical University, Department of Geology, Istanbul, Turkey, ⁵Yıldız Technical University, Department of Geomatics, Istanbul, Turkey, ⁶RSES, Australia National University, Canberra, Australia

Abstract During the past century, a series of predominantly westward migrating $M > 7$ earthquakes broke an ~ 1000 km section of the North Anatolian Fault (NAF). The only major remaining “seismic gap” along the fault is under the Sea of Marmara (Main Marmara Fault (MMF)). We use 20 years of GPS observations to estimate strain accumulation on fault segments in the Marmara Sea seismic gap. We report the first direct observations of strain accumulation on the Princes’ Islands segment of the MMF, constraining the slip deficit rate to 10–15 mm/yr. In contrast, the central segment of the MMF that was thought to be the most likely location for the anticipated gap-filling earthquakes shows no evidence of strain accumulation, suggesting that fault motion is accommodated by fault creep. We conclude that the Princes’ Islands segment is most likely to generate the next $M > 7$ earthquake along the Sea of Marmara segment of the NAF.

1. Introduction

The North Anatolian Fault (NAF) is a major right-lateral, strike-slip fault that extends more than 1200 km from eastern Turkey to the north Aegean Sea (Figure 1 inset) [Şengör *et al.*, 2005]. It accommodates the relative right-lateral motion between the Anatolian region and Eurasia at a geodetic rate of ~ 25 mm/yr [Meade *et al.*, 2002; Reilinger *et al.*, 2006]. Along its eastern and central sections, it is a relatively simple structure with almost pure strike-slip motion occurring on a single, clearly defined fault trace [Barka, 1996]. Along its westernmost segment, the fault bifurcates into northern and southern branches, the northern branch following Izmit Bay and entering the Sea of Marmara south east of Istanbul (Figure 1). By far the majority of long-term fault slip occurs on the northern fault branch following the northwest striking Princes’ Islands Fault (PIF) and joining the east-west striking Central Marmara Fault (CMF) immediately south of Istanbul [Le Pichon *et al.*, 2001; Armijo *et al.*, 2005]. After traversing much of the Sea of Marmara, the CMF merges with the Ganos Fault, exiting the Sea along the Ganos Peninsula (Figure 1).

During the twentieth century, the NAF failed in a remarkable sequence of major earthquakes that for the most part propagated from east to west (Figure 1 inset) [Toksöz *et al.*, 1979; Stein *et al.*, 1997]. The most recent major earthquake was the 1999, Izmit/Düzce earthquake pair with $M_w = 7.4/7.2$ that together broke a > 160 km segment of the fault [Armijo *et al.*, 2005]. The coseismic fault terminated on its western end, very near the eastern side of the Sea of Marmara. The Sea of Marmara segments (PIF and CMF) are the only ones that have not broken in major earthquakes during the twentieth century. Estimates of future gap-filling earthquakes suggest a high probability of imminent events with $M \geq 7.2$ [Le Pichon *et al.*, 2001; Parsons, 2004; Armijo *et al.*, 2005]. The Marmara segments are located close to the megacity of Istanbul with a rapidly growing population of > 13 million ($> 18\%$ of the country’s population) and the cultural, financial, and industrial heart of Turkey, adding important social implications for the geodetic constraints on strain accumulation presented in this study.

2. GPS Observations

Figure 1 shows the GPS velocity field for the Marmara region. Details of the GPS observations and tabulated rates and uncertainties are provided in Table S1 of the supporting information. The GPS data, acquired

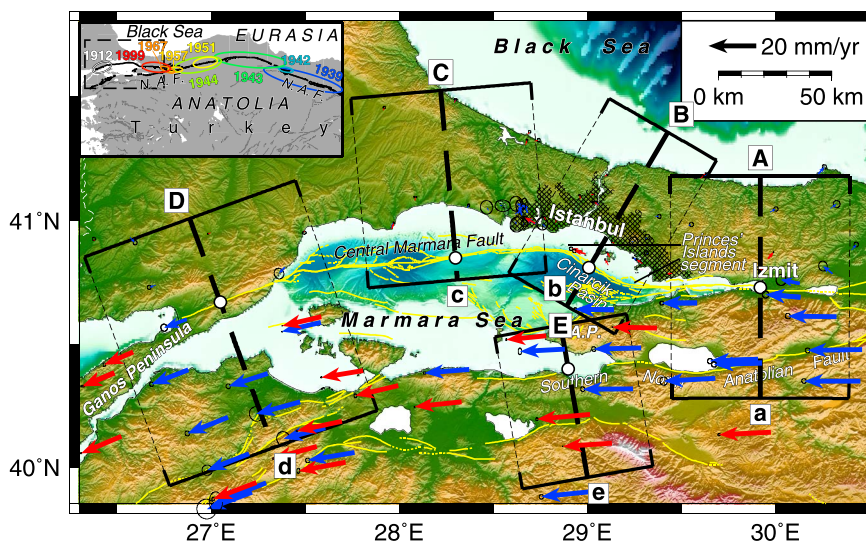


Figure 1. Sea of Marmara GPS velocities and 95% confidence ellipses plotted with respect to Eurasia (red = continuous station, blue = survey site). Locations of profiles shown in Figures 2a–2e (brackets indicate width), bathymetry, and faults (modified from Armijo *et al.* [2005]) are also indicated. The inset shows the twentieth century, westward propagating sequence of major earthquakes originating on the NAF (modified from Toksöz *et al.* [1979], Barka [1996], and Stein *et al.* [1997]).

over the past 20 years, were processed and velocities determined with the GAMIT/GLOBK software [Herring *et al.*, 2010] using standard procedures [Reilinger *et al.*, 2006], including the removal of coseismic offsets and estimation of annual and semiannual signals, and the addition of a random walk determined by first-order Gauss-Markov extrapolation (FOGMEX) [Herring, 2003; Reilinger *et al.*, 2006] to account for temporally correlated noise. We minimized the effects of postseismic deformation from the 1999 earthquakes by estimating and removing a logarithmic signal from the GPS position time series [Ergintav *et al.*, 2009].

3. GPS Velocity Field

Figures 2a–2e show plots of the GPS-derived velocities versus distance along the profiles shown in Figure 1. The profile perpendicular plots indicate strike-slip motion (bottom plots in Figures 2a–2e) and the profile parallel plots normal or thrust motion (top plots in Figures 2a–2e). The curves on the plots show strain accumulation models [Savage and Burford, 1973] for a vertical strike-slip fault in an elastic half space following the strike of the surface fault, locked from the surface to a range of depths and slipping freely below those depths at the rates indicated.

Profiles A and D cross the Izmit and Ganos segments respectively (Figure 1). They accommodate pure strike-slip motion (25 ± 2 and 20 ± 1 mm/yr). Profile B crosses the PIF segment along the eastern Sea of Marmara that extends northwest from near the end of the 1999 Izmit earthquake coseismic fault break to the CMF (Figure 1). Except for the one GPS site located on the Armutlu Peninsula 10 km southwest of the PIF, GPS velocities are confined to the northeast side of the fault. In addition to right-lateral offset across the PIF and Çınarcık basin (15 ± 2 mm/yr), the profile parallel velocity component (Figure 2b) indicates extension (6 ± 2 mm/yr) on, or southwest of the PIF. Profile C includes the full extent of the Central Marmara Fault that has little reported historical or instrumental seismicity (Figure 3). The sparse GPS velocity estimates along this segment provide upper bounds on fault slip rates on the eastern (south of Istanbul) and west-central segments of the fault (~2 mm/yr). Profile E crosses the eastern segment of the southern branch of the NAF. We observe right-lateral, strike-slip motion of 5 ± 2 mm/yr, although the spatial distribution is very poorly constrained.

The velocity plots crossing the Izmit and Ganos faults (Figures 2a and 2d) show spatially distributed motion indicative of a locked fault [Savage and Burford, 1973]. The estimated slip rates are well defined, insensitive to locking depth, and consistent with other published estimates [Meade *et al.*, 2002; Reilinger *et al.*, 2006;

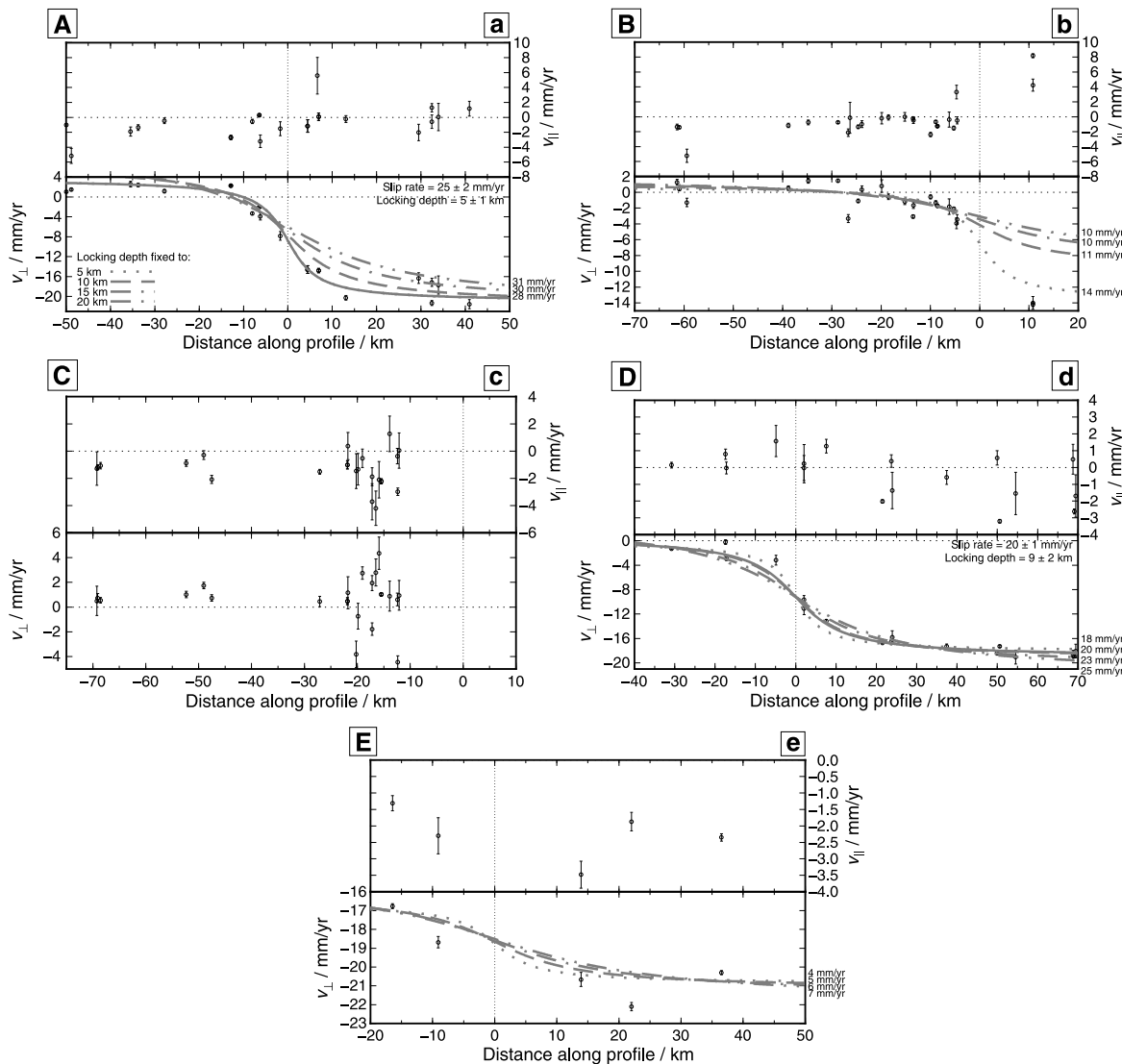


Figure 2. (a–e). GPS velocity plots showing the component of velocity parallel (top) and perpendicular (bottom) to the corresponding profiles shown in Figure 1 plotted versus perpendicular distance from the surface trace of the fault at the midsection of each profile. Since the profiles are oriented approximately perpendicular to the fault segments they cross, the top plots show the fault normal (thrusting or extension) and the bottom the fault-parallel (strike-slip) deformation rates. Curves show the deformation expected for an infinitely long, vertical strike-slip fault in an elastic half space [Savage and Burford, 1973] with deep slip rates estimated from the GPS observations indicated on the right for a range of locking depths (5–20 km; keyed in Profile A). Solid curves show the result of a simultaneous inversion for slip rate and locking depth where the data are sufficient to provide useful constraints (Figures 2a and 2d).

Hergert et al., 2011]. These segments of the NAF are known from instrumental and historic records to generate large earthquakes, the 1999 $M_w=7.4$, Izmit and the 1912 $M_w \sim 7.3$, Ganos earthquakes being the most recent (Figure 3).

GPS velocities northeast of the PIF segment indicate strike-slip strain accumulation (Figure 2b). Because the locking depth is very poorly constrained by the GPS observations (i.e., formal inversion gives $\sim 9 \pm 1$ mm/yr for strike-slip motion, $\sim 25 \pm 17$ km for locking depth. See Figure S1 in the supporting information), we estimate it at ~ 10 km from seismic observations [Bohnhoff et al., 2013] and a corresponding strike-slip rate for the PIF of $\sim 11 \pm 2$ mm/yr. The additional $\sim 6 \pm 2$ mm/yr of strike-slip motion indicated by the velocities on the Armutlu Peninsula (Figure 2b) could be due to any combination of a number of factors including (1) right-lateral strike slip on faults within or bounding the southern edge of the Cinarcik basin [Karabulut et al., 2002; Bulut et al., 2009; Karabulut et al., 2011], (2) asymmetric strain accumulation as a result of lower rigidity crust within the basin [Le Pichon et al., 2003; Huang and Johnson, 2012], or (3) a shallower locking

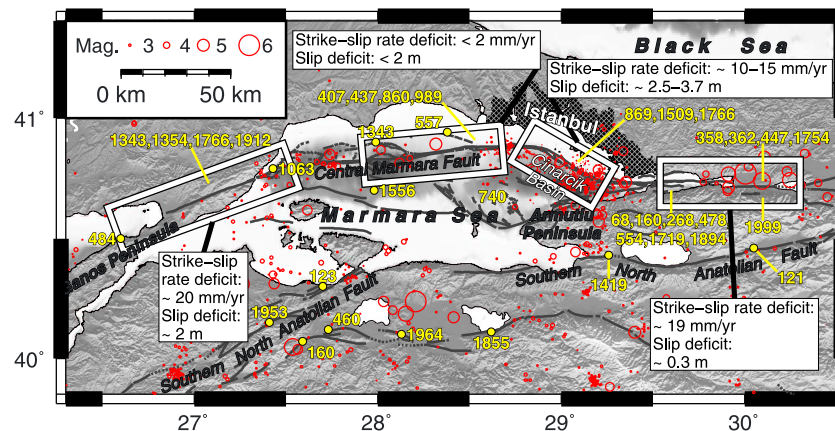


Figure 3. Map of historic earthquakes identified with particular fault segments in and around the Sea of Marmara (modified from Ambraseys [2002] and Pondard *et al.* [2007]). Faults [from Armijo *et al.*, 2005] and precisely located earthquakes (from Bohnhoff *et al.* [2013] and Tan *et al.* [2008]), and estimated slip rate deficits and the total deficits accumulated since the last major earthquakes are also shown.

depth for the PIF (Figure 2b). In addition to right-lateral strain accumulation, $\sim 6 \pm 2$ mm/yr of extension (Figure 2b) indicates dip-slip motion on the PIF and/or active normal faults within the basin [Le Pichon *et al.*, 2001; Karabulut *et al.*, 2002; Bulut *et al.*, 2009; Karabulut *et al.*, 2011].

4. Discussion and Implications for Earthquake Hazards

Historically, the PIF has been the most active in the Sea of Marmara (Figure 3). The most recent earthquake was the $M \sim 7.1$, 1766 event that caused loss of life and severe damage throughout Istanbul [Ambraseys, 2002]. If the profile perpendicular offset rate across the PIF segment ($\sim 15 \pm 2$ mm/yr, Figure 2b) is due entirely to strain accumulation on the PIF (i.e., no right-lateral slip on other faults in the Çınarcık basin), assuming a constant rate of strain accumulation, we estimate an upper bound of ~ 3.7 m for the slip deficit accumulated since the 1766 event. Our estimate of slip deficit rate for the PIF for a locking depth of ~ 10 km (11 ± 2 mm/yr), implies a lower bound for slip deficit of ~ 2.5 m. For the 50–60 km long PIF segment, these deficits would at present be sufficient to generate an earthquake with a magnitude comparable to the 1766 event [Wells and Coppersmith, 1994].

GPS observations north of the Sea of Marmara adjacent to the CMF show no indication of strain accumulation along this entire fault segment (Figure 2c and Figure S2 in the supporting information). The GPS velocities lie within a range of ± 2 mm/yr with no trend discernable even within these constraints, suggesting that the CMF may be failing via aseismic creep to shallow depths and hence may not be capable of generating large earthquakes [Meade *et al.*, 2002]. The elastic half-space models suggest an upper bound of ~ 2 mm/yr of strike-slip strain accumulation rate for a 10 km locking depth on this segment of the fault, at least in terms of its overall behavior. Low levels of strain accumulation support those interpretations of the historic earthquake record that report only two $M > 7$ earthquakes on the CMF in the past 2000 years, the largest being a $M \sim 7.2$ event in 989 AD along the eastern segment south of Istanbul and a $M \sim 7.0$ event located on the central segment in 1343 [Sengör *et al.*, 2005; Ambraseys, 2002; Pondard *et al.*, 2007]. Recent studies of earthquake-induced turbidite deposits provide further evidence that few large earthquakes have occurred in the past 2000 years on the CMF [McHugh *et al.*, 2014].

While present observations indicate low levels of strain accumulation on the CMF, GPS coverage along the north shore of the Sea of Marmara is sparse and only sufficient to constrain offset rates on the eastern and western segments of the fault. If no $M > 6.6$ earthquakes have occurred on the eastern segment in the past 1000 years as appears to be the case, it is possible that substantial strain has accumulated even at this low rate (~ 2 m; Figure 3). Similarly, in the 670 years since the 1343 event assigned to the western segment, ~ 1.5 m of slip deficit could have accumulated. Coseismic slip of 1–2 m would be expected to generate earthquakes in the magnitude range of 6.5–7.0 [Wells and Coppersmith, 1994].

5. Conclusions

The GPS velocity field around the Sea of Marmara indicates an internally consistent set of fault slip rates for the major branches of the westernmost NAF. Those branches that have generated $M > 7.1$ earthquakes as deduced from instrumental and historic earthquake studies are accumulating strain and are the most likely branches to generate future earthquakes (Figure 3). The Izmit and Ganos branches broke in large earthquakes in 1999 and 1912, and little strain is accumulating at present on both the eastern and western segments of the Central Marmara Fault, most likely due to aseismic fault creep to shallow levels, suggesting these segments have not had sufficient time to generate $M = 7$ events in the near future. In contrast, the PIF segment is actively accumulating strain and has not experienced a large event since 1766, making it the most likely segment to generate a $M > 7$ earthquake, and hence the most imminent seismic hazard to Istanbul and other cities around the Sea of Marmara. This result provides a physical basis for estimating the likely location, mechanism, and magnitude of the next major earthquake near Istanbul, information needed to develop more realistic earthquake scenarios for preparedness and response strategies, and for undertaking future investigations to further evaluate subsea fault behavior.

Acknowledgments

We thank UNAVCO for technical assistance with the GPS observations and the many individuals who contributed to GPS measurements around the Sea of Marmara during the past 20 years. We are grateful to Marco Bohnhoff and an anonymous reviewer for their helpful reviews. This study has been partially supported by TUBITAK projects 103Y100, 108Y152, and 105G019, B.U. Research Funds with grant 7685, NSF grants EAR-0838488, 1045487, and 1246577 to MIT, and EU-FP7 grant agreement 308417 to Boğaziçi University. Most figures are drawn with GMT [Wessel and Smith, 1998]. We have used GPS data in the public domain (UNAVCO, IGS, and EUREF) and in the supporting information of the previously published studies. We also, have been given the calculated velocity field in the supporting information of this manuscript.

The Editor thanks Marco Bohnhoff and an anonymous reviewer for their assistance in evaluating this paper.

References

- Ambraseys, N. (2002), The seismic activity of the Marmara Sea region over the last 2000 years, *Bull. Seismol. Soc. Am.*, 92, 1–18.
- Armijo, R., et al. (2005), Submarine fault scarps in the Sea of Marmara pull-apart (North Anatolian Fault): Implications for seismic hazard in Istanbul, *Geochem. Geophys. Geosyst.*, 6, Q06009, doi:10.1029/2004GC000896.
- Barka, A. (1996), Slip distribution along the North Anatolian Fault associated with large earthquakes of the period 1939–1967, *Seismol. Soc. Am. Bull.*, 86, 1238–1254.
- Bohnhoff, M., F. Bulut, G. Dresen, P. E. Malin, T. Eken, and M. Aktar (2013), An earthquake gap south of Istanbul, *Nature*, doi:10.1038/ncomms2999.
- Bulut, F., M. Bohnhoff, W. L. Ellsworth, M. Aktar and G. Dresen, (2009), Microseismicity at the North Anatolian Fault in the Sea of Marmara offshore Istanbul, NW Turkey, *J. Geophys. Res.*, 114, B09302, doi:10.1029/2008JB006244.
- Ergintav, S., S. McClusky, E. Hearn, R. Reilinger, R. Cakmak, T. Herring, H. Ozener, O. Lenk, and E. Tari (2009), Seven years of postseismic deformation following the 1999, $M = 7.4$ and $M = 7.2$ Izmit-Duzce, Turkey earthquake sequence, *J. Geophys. Res.*, 114, B07403, doi:10.1029/2008JB006021.
- Hergert, T., O. Heidbach, A. Becel, and M. Laigle (2011), Geomechanical model of the Marmara Sea region—1. 3-D contemporary kinematics, *Geophys. J. Int.*, 185, 1073–1089.
- Herring, T. (2003), MATLAB tools for viewing GPS velocities and time series, *GPS Solutions*, 7(3), 194–199.
- Herring, T. A., R. W. King, and S. McClusky (2010), *Introduction to GAMIT/GLOBK, Release 10.4*, MIT Press, Cambridge, Mass.
- Huang, W. J., and K. M. Johnson (2012), Strain accumulation across strike-slip faults: Investigation of the influence of laterally varying lithospheric properties, *J. Geophys. Res.*, 117, B09407, doi:10.1029/2012JB009424.
- Karabulut, H., M.-P. Bouin, M. Bouchon, M. Dietrich, C. Cornou, and M. Aktar (2002), The seismicity of the eastern Marmara Sea after the 17 August 1999 Izmit earthquake, *Bull. Seismol. Soc. Am.*, 92, 387–393.
- Karabulut, H., J. Schmittbuhl, S. Özalaybey, O. Lengliné, A. Kömeç-Mutlu, V. Durand, M. Bouchon, G. Daniel, and M. P. Bouin (2011), Evolution of the seismicity in the eastern Marmara Sea a decade before and after the 17 August 1999 Izmit earthquake, *Tectonophysics*, 510, 17–27.
- Le Pichon, X., A. M. C. Sengör, E. Demirbag, C. Rangin, C. Imren, R. Armijo, N. Gorur, and N. Cagatay (2001), The active Main Marmara Fault, *Earth Planet. Sci. Lett.*, 192, 595–616.
- Le Pichon, X., N. Rangin, C. Chamot-Rooke, and A. M. C. Sengör (2003), The North Anatolian Fault in the Sea of Marmara, *J. Geophys. Res.*, 108(B4), 2179, doi:10.1029/2002JB001862.
- McHugh, C. M. G., N. Braud, M. N. Çağatay, C. Sorlien, M.-H. Cormier, L. Seeber, and P. Henry (2014), Seafloor fault ruptures along the North Anatolia Fault in the Marmara Sea, Turkey: Link with the adjacent basin turbidite record, *Mar. Geol.*, 353, 65–83.
- Meade, B. J., B. H. Hager, S. C. McClusky, R. E. Reilinger, S. Ergintav, O. Lenk, A. Barka, and H. Ozener (2002), Estimates of seismic potential in the Marmara region from block models of secular deformation constrained by GPS measurements, *Bull. Seismol. Soc. Am.*, 92, 208–215.
- Parsons, T. (2004), Recalculated probability of $M 7$ earthquakes beneath the Sea of Marmara, Turkey, *J. Geophys. Res.*, 109, B05304, doi:10.1029/2003JB002667.
- Pondard, N., R. Armijo, G. C. P. King, B. Meyer, and F. Flerit (2007), Fault interactions in the Sea of Marmara pull-apart (North Anatolian Fault): Earthquake clustering and propagating earthquake sequences, *Geophys. J. Int.*, 171(3), 1185–1197.
- Reilinger, R., et al. (2006), GPS constraints on continental deformation in the Africa-Arabia-Eurasia continental collision zone and implications for the dynamics of plate interactions, *J. Geophys. Res.*, 111, B05411, doi:10.1029/2005JB004051.
- Savage, J. C., and J. L. Burford (1973), Geodetic deformation of relative plate motion in central California, *J. Geophys. Res.*, 78, 832–845, doi:10.1029/JB078i005p00832.
- Sengör, A. M. C., O. Tuysuz, C. Imren, M. Sakinc, H. Eyidogan, N. Gorur, X. Le Pichon, and C. Rangin (2005), The North Anatolian fault: A new look, *Annu. Rev. Earth Planet. Sci.*, 33, 37–112.
- Stein, R. S., A. Barka, and J. D. Dieterich (1997), Progressive failure on the North Anatolian fault since 1939 by earthquake stress triggering, *Geophys. J. Int.*, 128, 594–604.
- Tan, O., M. C. Tapirdamaz, and A. Yörük (2008), The earthquake catalogues for Turkey, *Turkish J. Earth Sci.*, 17, 405–418.
- Toksöz, M. N., A. F. Shakal, and A. J. Michael (1979), Space-time migration of earthquakes along the North Anatolian Fault and seismic gaps, *Pure Appl. Geophys.*, 117, 1258.
- Wells, D. L., and K. J. Coppersmith (1994), Empirical relationships between magnitude, rupture length, rupture width, rupture area and surface displacement, *Bull. Seismol. Soc. Am.*, 84, 974–1002.
- Wessel, P., and W. H. F. Smith (1998), New, improved version of the generic mapping tools released, *Eos. Trans. AGU*, 79, 579, doi:10.1029/98EO00426.

Erratum

In the originally published version of this article, author Z. Cakir's name was misspelled. It has since been corrected, and this version may be considered the authoritative version of record.